

Notes and a few figures for discussion of  $\mu$ -bar *vs.*  $E$   
for neutron elastic scattering on actinides *at low energies*

D. Roubtsov, K. Kozier  
CRL, AECL, Canada  
December 2010

See presentations of T. Kawano, CSEWG-2010 (in Santa Fe, NM)

<http://www.nndc.bnl.gov/proceedings/2010csewgusndp/Thursday/AFCIP/modscat-Kawano.pdf>

and at WINS-2010 (Strasbourg).

In a typical ENDF/B file, for MT=2 (*i.e.*, for the elastic scattering channel of  $n + A$ ), there are two data blocks: MF=3, MT=2 for the scattering cross sections,  $\sigma_s(E)$ , and MF=4, MT=2 for the scattering angular distributions,  $P_s(E, \mu)$ , usually given in the CM-frame and normalized to one,  $\int_{-1}^1 P_s(E, \mu) d\mu = 1$ .

For heavy elements, CM- and LAB-frames of  $n + A \rightarrow n + A$  are almost indistinguishable, *i.e.*,

$$P_s^{(\text{CM})}(E, \mu_{\text{CM}}) \approx P_s^{(\text{LAB})}(E, \mu_{\text{LAB}}).$$

Then, the elastic scattering differential cross section,  $d\sigma_s(E, \mu)/d\Omega$ , can be written as

$$d\sigma_s(E, \mu)/d\Omega = \sigma_s(E) \times P_s(E, \mu)/2\pi, \text{ in [ b/sr ].}$$

There is **no** MF=6, MT=2 data block for  $d^2\sigma_s(E \rightarrow E', \mu)/dE'd\Omega$  in ENDF/B files because

$$d^2\sigma_s(E \rightarrow E', \mu)/dE'd\Omega = \sigma_s(E) \times P_s(E, E', \mu)/2\pi = \sigma_s(E) \times P_s(E, \mu) \times P_s(E \rightarrow E')/2\pi,$$

*i.e.*,  $P_s(E, E', \mu) = P_s(E, \mu) P_s(E \rightarrow E')$ . It is assumed that the energy distribution of elastic scattering  $P_s(E \rightarrow E')$  is independent of  $\mu$  and it follows from the kinematics (in the limit  $T \rightarrow 0$  K). As  $P_s(E, \mu)$  is normalized to unity, the average scattering cosine of neutron elastic scattering,  $\mu\text{-bar}$ , can be calculated as follows:

$$\mu\text{-bar} = \iint \mu \times d^2\sigma_s(E \rightarrow E', \mu)/dE'd\Omega / \iint d^2\sigma_s(E \rightarrow E', \mu)/dE'd\Omega = \int_{-1}^1 \mu \times P_s(E, \mu) d\mu.$$

Assume that a given ENDF/B file was processed by NJOY99 into a **fast** ACE file corresponding to a given temperature  $T$  ( $\neq 0$  K). Then,  $\sigma_s(E)$  is Doppler broadened,  $\sigma_s(E) \rightarrow \sigma_s(E; T)$ , using the resonance parameters from MF = 2 (if any).

**What happens with  $P_s(E, \mu)$ ?**

In other words, how does **NJOY99** process **MF=4, MT=2** data for **MCNP(X)** ?

If  $P_s(E, \mu)$  is given in the form of tables, *i.e.*, for each  $E_j$ , there is a table of  $k$  entities,

$$(\mu_{jk}, P_{s,jk}), -1.0 \leq \mu_{jk} \leq 1.0,$$

then these data points are transferred to the fast ACE file *as they are* in the original ENDF/B file. Thus, NJOY99 does the following transformation:

$$\text{ENDF/B MF=4, MT=2 } (E_j, \mu_{jk}, P_{s,jk}) \rightarrow \text{ACE } (E_j, \mu_{jk}, P_{s,jk}, P_{s,jk}^c). \quad (1)$$

Here,  $P_{s,jk}^c$  is the cumulative angular distribution,  $P_s^c(E, \mu) = \int_{-1}^{\mu} P_s(E, \mu') d\mu'$ .

Note that there are **no changes**: the same grids for  $E_j$  and for  $\mu_{jk}$  are in both ENDF/B MF=4, MT=2 and in the corresponding ACE part, and  $P_{s,jk}$  and  $P_{s,jk}^c$  are independent on temperature  $T$ .

If  $P_s(E, \mu)$  is given in the form of Legendre polynomial expansion, *i.e.*, for each  $E_j$ , there is a ‘vector’ of coefficients,

$$a_{s,jl}, \quad l = 1, \dots, l_{\max,j},$$

then **acer** module of NJOY99 [ptleg2] converts vectors  $a_{s,jl}$  into tables  $(\mu_{jk}, P_{s,jk})$  by choosing an **optimal grid** of the scattering cosines  $\mu_{jk}$  (for each  $E_j$ ) and applying

$$P_{s,jk} = 1/2 + \sum_{l=1} ((2l+1)/2) \times a_{s,jl} \times P_l(\mu_{jk}).$$

Therefore, NJOY99 does the following transformation:

$$\text{ENDF/B MF=4, MT=2 } (E_j, a_{s,jl}, l_{\max,j}) \rightarrow \text{ACE } (E_j, \mu_{jk}, P_{s,jk}, P_{s,jk}^c). \quad (2)$$

Note that the same grid  $E_j$  is in both ENDF/B MF=4, MT=2 and in the corresponding ACE part, and  $P_{s,jk}$  and  $P_{s,jk}^c$  are independent on  $T$ .

As  $P_1(\mu) = \mu$ , the coefficient  $a_{s,j1}$  ( $l = 1$ ) is the  $\mu$ -bar for neutron elastic scattering at  $E_j$ ,

$$\mu\text{-bar}(E_j) = a_{s,j1}.$$

$P_s^c(E, \mu)$  data given in ACE files are useful to estimate the integral backward-to-forward scattering ratio (B2FR) *vs.*  $E$  (in the CM frame, strictly speaking):

$$\text{B2FR} = \int_{-1}^0 P_s(E, \mu) d\mu / \int_0^1 P_s(E, \mu) d\mu = P_s^c(E, \mu = 0) / (1 - P_s^c(E, \mu = 0)).$$

One can check Figures given at <https://t2.lanl.gov/nis/data/endl/endlfvii-n.html> under “view PDF plots”. These plots are visualization of the typical results obtained by processing of a given ENDF/B file of ENDF/B-VII.0 into a fast ACE file (at room temperature) with NJOY99.

For  $^{238}\text{U}$ , check Figure 36 (page 36), subtitle “*angular distribution for elastic*”: this is  $P_s(E, \mu)$  plotted from the data block  $(E_j, \mu_{jk}, P_{s,jk})$  calculated/processed by **NJOY99** (**acer**) from the original MF=4, MT=2 of  $^{238}\text{U}$ .

Below, we show a similar figure for  $P_s(E, \mu)$  of  $^{238}\text{U}$  obtained from an ACER output in the energy region  $1\text{eV} < E < 1.0\text{ MeV}$ . We used JENDL 4.0  $^{238}\text{U}$  because MF=4, MT=2 of this file has a better (denser)  $E_j$  grid for visualization of  $P_s(E, \mu)$  at low energies.

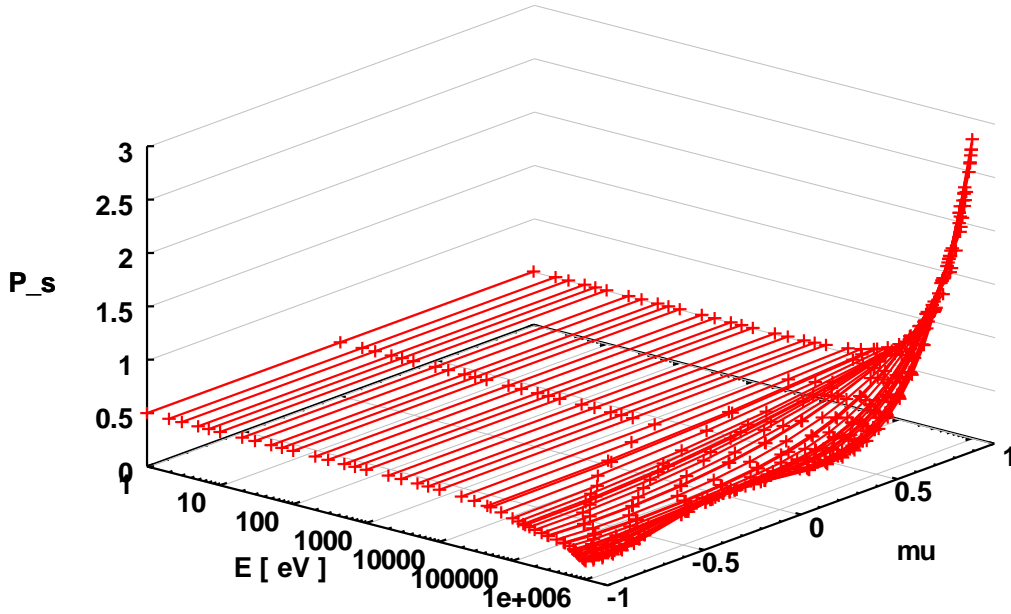


**Fig. 1:**  $P_s(E, \mu)$  of  $^{238}\text{U}$  (JENDL 4.0),  $1.0 \text{ eV} < E < 1.0 \text{ MeV}$ .

Conversion from  $(E_j, a_{s,jl})$  to  $(E_j, \mu_{jk}, P_{s,jk})$  and selection of optimal  $\mu_{jk}$  are done by **acer** module of NJOY99. For example,  $\dim_k(\mu_{jk}) = 3$  for  $E_j \leq 20.0 \text{ keV}$ .

As follows from Fig. 1, in the Resolved Resonance Energy Region,  $E < 20 \text{ keV}$  (ENDF/B-VII.0), one can use **P1** approximation for  $P_s(E, \mu)$  of  $^{238}\text{U}$ :

$$P_s(E, \mu) \approx 1/2 + (3/2) \times \mu\text{-bar}(E) \times \mu.$$

$\mu\text{-bar}(E)$  for  $^{238}\text{U}$  is given in Fig. 2 for low neutron energies,  $1 \text{ eV} < E < 0.3 \text{ MeV}$ .

We did not find experimental data for  $d\sigma_s(E, \mu)/d\Omega$  or  $P_s(E, \mu)$  of  $^{238}\text{U}$  at the incident energies  $E$  lying in the  $^{238}\text{U}$  **RRR** in EXFOR database. The lowest energy data sets that we noticed are

$E = 55 \text{ keV}$  by Murzin-1987 and  $E = 75 \text{ keV}$  by Barnard-1966, then  $E \approx 150 \text{ keV}$ , *etc.*, *i.e.*, the lowest energies are lying in the  $^{238}\text{U}$  **URR**. (EXFOR search: U-238; n,\*; DA.)

Note that, at  $E > 50\text{-}100 \text{ keV}$ , the **inelastic** scattering channels with excitation of the lowest levels of  $^{238}\text{U}$  open up.

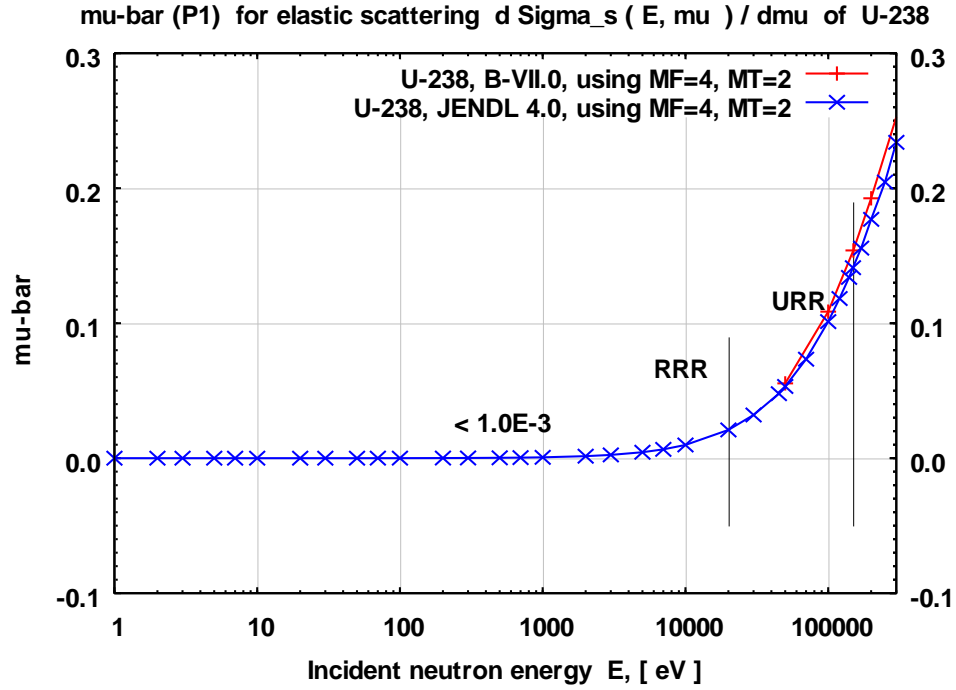


**Fig. 2:**  $\mu\text{-bar}(E)$  for  $^{238}\text{U}$ ;  $\mu\text{-bar}(E) < 10^{-3}$  at  $E < 1\text{--}2$  keV;  
 RRR boundary: 20 keV, URR boundary: 149 keV (ENDF/B-VII.0).  
 (In ENDF/B-VII.0, the grid starts as  $E_1 = 10^{-5}$  eV,  $E_2 = 50$  keV, ... in MF=4, MT=2 of  $^{238}\text{U}$ .)

Similar results can be obtained for  $^{232}\text{Th}$ .

As follows from Fig. 3, in the Resolved Resonance Energy Region,  $E < 4$  keV (ENDF/B-VII.0), one can use P1 approximation for  $P_s(E, \mu)$  of  $^{232}\text{Th}$ :

$$P_s(E, \mu) \approx 1/2 + (3/2) \times \mu\text{-bar}(E) \times \mu.$$

$\mu\text{-bar}(E)$  for  $^{232}\text{Th}$  is given in Fig. 4 for low neutron energies,  $1 \text{ eV} < E < 0.3 \text{ MeV}$ .

Similarly, we did not find experimental data for  $d\sigma_s(E, \mu)/d\Omega$  or  $P_s(E, \mu)$  of  $^{232}\text{Th}$  at the incident energies  $E$  in the  $^{232}\text{Th}$  **RRR** in EXFOR database.

The angular distribution data in EXFOR are at  $E > 100$  keV, *i.e.*, they are even outside  $^{232}\text{Th}$  URR (and at the incident neutron energies at which the inelastic scattering channels open up).

EXFOR search: Th-232; n,\*; DA.

There is a paper by Samosvat-1970, "ANGULAR DISTRIBUTIONS OF SCATTERING OF 1-40 KEV NEUTRONS" with Legendre coefficients ( $a_{s,jl}$  ?) and  $E_{\min} = 1.6$  keV.

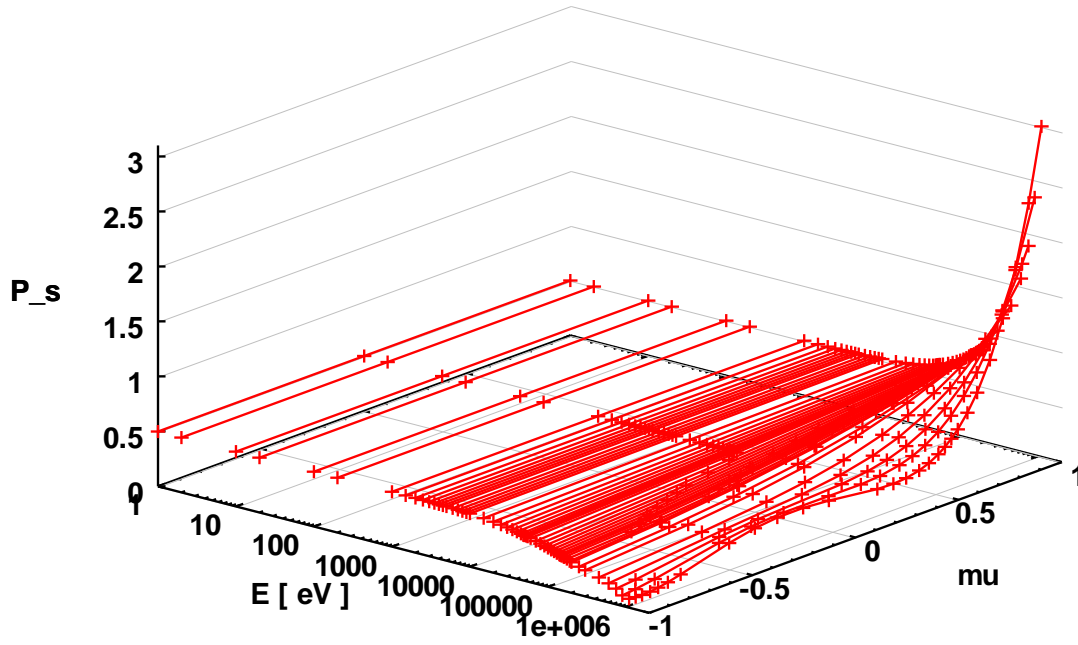


**Fig. 3:**  $P_s(E, \mu)$  of  $^{232}\text{Th}$  (ENDF/B-VII.0),  $1\text{eV} < E < 1.0\text{ MeV}$ .

Conversion from  $(E_j, a_{s,jl})$  to  $(E_j, \mu_{jk}, P_{s,jk})$  and selection of optimal  $\mu_{jk}$  are done by **acer** module of NJOY99. For example,  $\dim_k(\mu_{jk}) = 3$  for  $E_j \leq 60\text{ keV}$ .

(We added a few  $E_j$  between the original grid points,  $E_1 = 10^{-5}\text{ eV}$  and  $E_2 = 1.0\text{ keV}$  of MF=4, MT=2 of  $^{232}\text{Th}$  to improve visual perception).

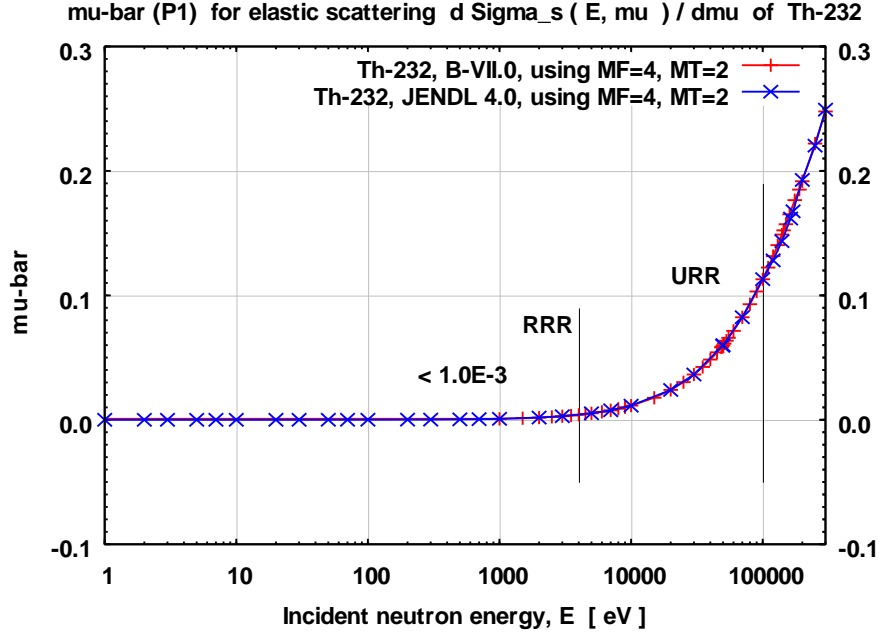


**Fig. 4:**  $\mu\text{-bar}(E)$  for  $^{232}\text{Th}$ ;  $\mu\text{-bar}(E) < 10^{-3}$  at  $E < 1.0\text{-}1.5$  keV.  
 RRR boundary: 4 keV, URR boundary: 100 keV (ENDF/B-VII.0).  
 (In ENDF/B-VII.0, the grid starts as  $E_1 = 10^{-5}$  eV,  $E_2 = 1.0$  keV in MF=4, MT=2 of  $^{232}\text{Th}$ .)

In Fig. 5, we show the resonance behavior of  $\sigma_s(E)$  and  $\sigma_{n,\gamma}(E)$  for  $^{238}\text{U}$  and  $^{232}\text{Th}$  at low energies,  $1 \text{ eV} < E < 1 \text{ keV}$ . As  $\sigma_s$  vs.  $E$  has a pronounced **s-wave** resonance character at low energies, we have, roughly,

$$P_s(E, \mu) \approx 1/2,$$

*i.e.*, nearly isotropic angular scattering distributions at low energies  $E < 1$  keV for  $n + ^{238}\text{U}$  and  $n + ^{232}\text{Th}$ .

(**p-wave** resonances contribute to  $\sigma_s(E)$  at  $E > 1$  keV, roughly.)

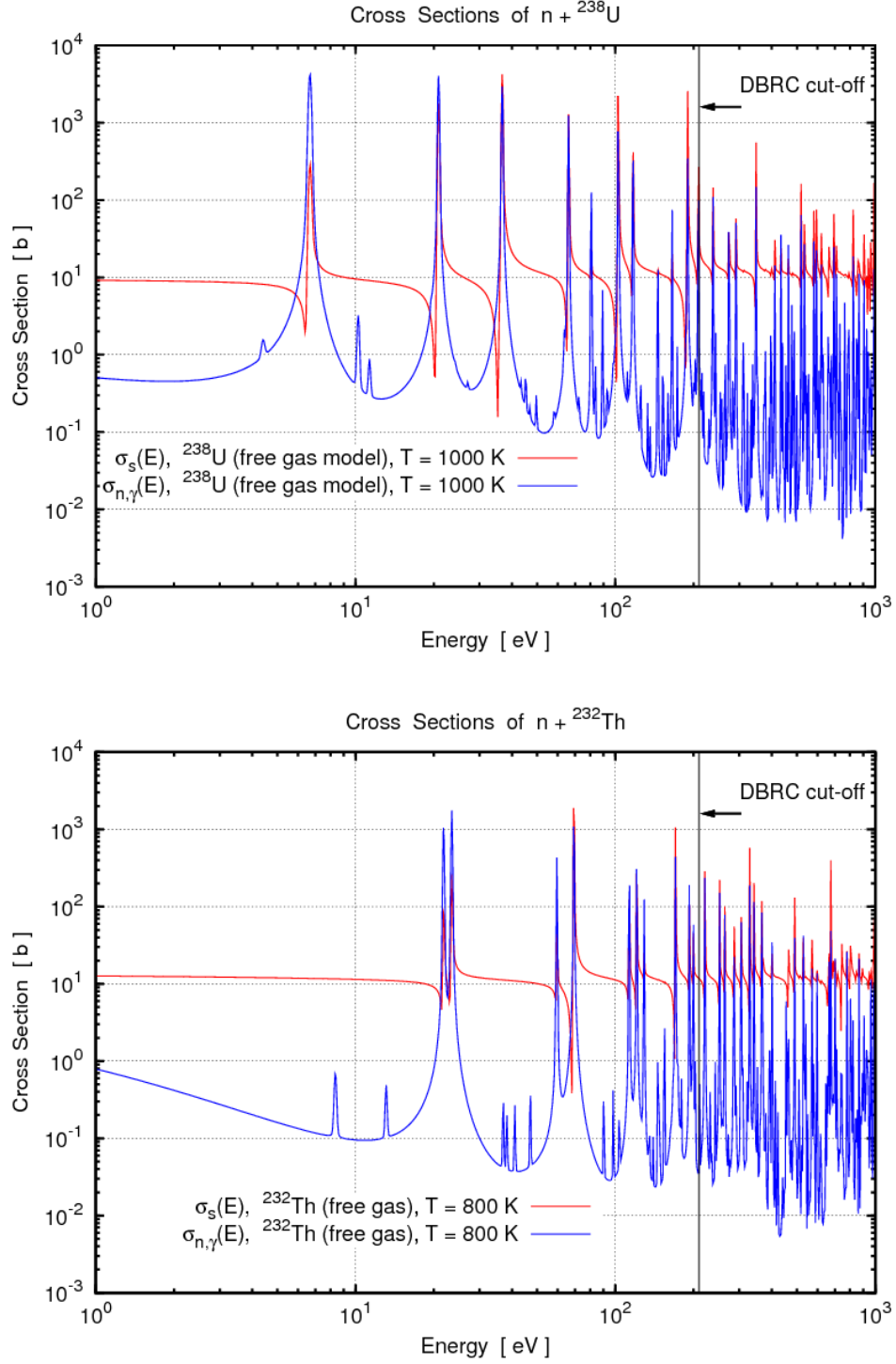


**Fig. 5:** low-lying neutron resonances of  ${}^{238}\text{U}$  and  ${}^{232}\text{Th}$  (ENDF/B-VII.0, NJOY99) at  $1\text{ eV} < E < 1\text{ keV}$ . Almost all the low-lying **scattering** resonances of  $\sigma_s(E)$  are *s*-wave type and  $\mu\text{-bar}(E) < 10^{-3}$  at  $E < 1.0\text{ keV}$ . (DBRC cut-off = 210.0 eV, R. Dagan).